JCI insight

RESEARCH ARTICLE

Symptomatic treatment of botulism with a clinically approved small molecule

Edwin Vazquez-Cintron, James Machamer, Celinia Ondeck, Kathleen Pagarigan, Brittany Winner, Paige Bodner, Kyle Kelly, M. Ross Pennington, and Patrick McNutt

Department of Neuroscience, U.S. Army Medical Research Institute of Chemical Defense, Gunpowder, Maryland, USA.

Botulinum neurotoxins (BoNTs) are potent neuroparalytic toxins that cause mortality through respiratory paralysis. The approved medical countermeasure for BoNT poisoning is infusion of antitoxin immunoglobulins. However, antitoxins have poor therapeutic efficacy in symptomatic patients; thus, there is an urgent need for treatments that reduce the need for artificial ventilation. We report that the US Food and Drug Administration–approved potassium channel blocker 3,4-diaminopyridine (3,4-DAP) reverses respiratory depression and neuromuscular weakness in murine models of acute and chronic botulism. In ex vivo studies, 3,4-DAP restored end-plate potentials and twitch contractions of diaphragms isolated from mice at terminal stages of BoNT serotype A (BoNT/A) botulism. In vivo, human-equivalent doses of 3,4-DAP reversed signs of severe respiratory depression and restored mobility in BoNT/A-intoxicated mice at terminal stages of respiratory collapse. Multiple-dosing administration of 3,4-DAP improved respiration and extended survival at up to 5 LD_{50} BoNT/A. Finally, 3,4-DAP reduced gastrocnemius muscle paralysis and reversed respiratory depression in sublethal models of serotype A–, B–, and E–induced botulism. These findings make a compelling argument for repurposing 3,4-DAP to symptomatically treat symptoms of muscle paralysis caused by botulism, independent of serotype. Furthermore, they suggest that 3,4-DAP is effective for a range of botulism symptoms at clinically relevant time points.

Introduction

Botulinum neurotoxins (BoNTs) are a family of potent protein neurotoxins naturally expressed by members of the *Clostridium* genus of anaerobic bacteria (1). BoNTs are the most poisonous substances known, with estimated human median lethal dose (LD_{50}) values as low as 0.1–1 ng/kg (2). BoNTs are categorized into 7 canonical antigenic serotypes (A–G) and further stratified into over 40 subtypes based on primary sequence divergence (3). The therapeutic challenge presented by this diversity is compounded by the ongoing discovery of noncanonical serotypes and subtypes with unknown toxicokinetic properties, as well as genetic engineering of existing toxins to introduce capabilities (4). BoNT has a characteristic heterodimeric protein structure consisting of a 100-kDa heavy chain (HC) and 50-kDa light chain (LC), which are associated through a disulfide bond. HC mediates highly selective and efficient binding to endosomal receptors on the presynaptic membrane of peripheral neurons (5, 6). Following internalization via synaptic endocytosis, LC translocates across the endosomal membrane to the presynaptic cytosol, where it specifically cleaves neuronal SNARE (soluble *N*-ethylmaleimide–sensitive factor attachment protein receptor) proteins essential for neurotransmitter exocytosis (2). Cleavage of SNAP25 by serotypes A, C, or E; SYB1–3 by serotypes B, D, F, and G; or STX1 by serotype C inhibits assembly of the SNARE protein complex that mediates synaptic vesicle fusion with the presynaptic membrane, thereby preventing neurotransmitter release (7, 8).

The clinical syndrome of botulism results from peripheral blockade of neurotransmission at neuromuscular junctions, autonomic ganglia, and parasympathetic and sympathetic nerve endings (9). Depending on the toxic dose, early symptoms of exposure manifest within 12–72 hours as cranial nerve dysfunctions (10). In mild cases, these symptoms fully resolve, but in severe cases, life-threatening symptoms of botulism emerge, including descending flaccid muscle paralysis and respiratory failure. At lethal doses, patient survival requires intensive care with parenteral feeding and artificial ventilation. Because many BoNT serotypes exhibit prolonged persistence within the nerve terminal, recovery

Conflict of interest: The authors have declared that no conflict of interest exists.

Submitted: August 26, 2019
Accepted: December 18, 2019
Published: January 30, 2020.

Reference information: *JCI Insight*. 2020;5(2):e132891. https://doi.org/10.1172/jci.insight.132891.

from lethal doses may require months, during which respiratory support must be continuously sustained and patients remain at risk for life-threatening comorbidities (11–13). Recovery of neuromuscular function occurs once LC activity is eliminated, cleaved SNARE proteins have been replaced with intact SNARE proteins, and functional motor end-plates have regenerated (if atrophy has occurred). While victims of lethal exposures are likely to survive if provided sustained respiratory support, recovery of normal neurological function can be protracted or never fully occur (14).

Based on the molecular and cellular toxicokinetics of intoxication (15), a comprehensive therapeutic paradigm for botulism would include (a) broad-spectrum antitoxins to terminate exposure, (b) intracellular antidotes to block LC proteolysis of SNARE proteins, and (c) symptomatic treatments that enhance neuromuscular function and mitigate muscle weakness, with mechanical ventilation administered as needed to ensure survival. However, the only approved treatment for botulism is antitoxin, which neutralizes BoNTs in the bloodstream and prevents further neuronal uptake (16). Due to the profound acute toxicity of BoNT, antitoxin efficacy is critically dependent on time of administration after exposure (17–19). The majority of botulism patients given antitoxin after symptomatic onset require mechanical ventilation for survival, even if antitoxins are administered within 48 hours of symptomatic emergence (13, 20, 21). Thus, there remains a critical need for complementary therapies that promote respiratory function and reduce or eliminate the need for ventilation.

It has been proposed that neuromuscular paralysis can be overcome by drugs that increase cholinergic neurotransmission (22, 23). Indeed, we and other groups have shown that aminopyridines such as 3,4-diaminopyridine (3,4-DAP) transiently reverse muscle paralysis in a concentration-dependent manner (24–27). 3,4-DAP is a selective potassium channel blocker that prolongs neuronal action potential duration, thereby increasing Ca^{2+} influx through presynaptic voltage-gated Ca^{2+} channels (28–30). Because vesicle fusion is steeply dependent on Ca^{2+} levels, 3,4-DAP increases release probability and release of acetylcholine (24, 31, 32). However, aminopyridines have had variable efficacies in treating botulism signs and symptoms in preclinical and clinical studies, raising concerns about their efficacy and mechanism of action. For example, aminopyridines have been described to be both effective (33, 34) and ineffective (35) in reversing toxic signs of type C botulism in rats. While 3,4-DAP is widely described as effective in treating type A botulism paralysis and prolonging survival in rodent studies (25, 27, 36), clinical studies variably indicate symptomatic benefit (37) or lack of benefit (38). Similarly, whereas 3,4-DAP has been reported to be ineffective in treating serotype B botulism in rodents (25, 39, 40), robust therapeutic efficacy was demonstrated in a clinical case of serotype B botulism involving mechanical ventilation (41).

Mechanistic studies conducted in BoNT-intoxicated primary neuron cultures and mouse diaphragms demonstrate that 3,4-DAP has multiple effects on the function of intoxicated nerve terminals, providing a plausible explanation for these variable clinical outcomes. First, 3,4-DAP increases quantal content of end-plates by serotypes A, B, or E (24). This effect becomes less robust as end-plates are increasingly paralyzed, indicating that 3,4-DAP works by increasing the probability of vesicle fusion at intact release sites (i.e., release sites not associated with cleaved SNARE proteins). Second, 3,4-DAP uniquely restores neurotransmission to synapses and neuromuscular junctions fully blocked by BoNT serotype A (BoNT/A) (24, 42). This indicates that 3,4-DAP will have increased efficacy against type A botulism, which comprises approximately 50% of botulism cases in the United States (43). Collectively, these findings suggest that 3,4-DAP could be effective as a symptomatic treatment for clinical botulism at multiple time points, independent of serotype, and with enhanced potency in cases of type A botulism.

Here, we test the hypothesis that 3,4-DAP improves respiratory and skeletal muscle paralysis in vivo at clinically relevant time points after exposure to BoNT serotypes A, B, and E. These studies were conducted in mice intoxicated with up to 5 LD_{50} of toxin. Based on correlation of the rate of disease progression between nonhuman primates and clinical patients, 5 LD_{50} is estimated to represent an upper range for typical human foodborne exposure to serotypes A, B, or E (44, 45). We found that human-equivalent doses of 3,4-DAP reversed limb and respiratory paralysis caused by each BoNT serotype. Therapeutic efficacy was most robust during recovery from botulism versus peak paralysis. However, 3,4-DAP was uniquely able to reverse terminal respiratory depression and prolong survival in mice lethally intoxicated with up to 5 LD_{50} BoNT/A. Collectively, these results make a compelling argument for the clinical evaluation of 3,4-DAP to reduce morbidity and mortality associated with acute and chronic symptoms of botulism.

Results

DAP reverses neurotransmission failure in diaphragms isolated from BoNT/A-intoxicated mice. We previously reported that 3,4-DAP increased nerve-elicited end-plate potentials (EPP) and twitch contraction amplitudes in hemidiaphragm preparations paralyzed by BoNT serotypes A, B, or E (24). These studies involved bath intoxication with supraphysiological toxin concentrations to achieve full paralysis during the viable window of diaphragm preparations. To determine whether 3,4-DAP improved neurotransmission in diaphragm end-plates following a physiological intoxication, phrenic nerve–diaphragm preparations were isolated at 16–20 hours after i.p. injection of 2 LD_{50} BoNT/A, and the effects of 3,4-DAP on end-plate function were analyzed using muscle contraction studies and intracellular recordings. At euthanasia, mice presented with generalized muscle weakness, paradoxical abdominal breathing, and agonal respiration, indicating recruitment of accessory respiratory muscles to compensate for diaphragm paralysis (46). In comparison with naive controls, intoxicated end-plates exhibited a 98.7% reduction in the frequency of spontaneous miniature EPPs (mEPPs; 0.01 ± 0.01 versus 1.10 ± 0.11 Hz; $n = 5$ each, $P < 0.0001$, Welch's t test) and 99.6% reduction in the area of EPPs (0.24 ± 0.03 versus 64.85 ± 6.62 mV·ms; Figure 1, A and B). Addition of 10 μM 3,4-DAP increased EPP area by 130-fold (0.24 ± 0.03 to 31.4 ± 3.8 mV·ms), restoring EPPs to nearly 50% of naive values. In muscle function studies, addition of 10 μM 3,4-DAP increased nerve-elicited twitch contraction strengths of intoxicated diaphragms by 6-fold (0.25 ± 0.08 to 1.71 ± 0.34 g; Figure 1, C and D). 3,4-DAP enhancement of EPPs and muscle contraction was fully reversed after washout, demonstrating that 3,4-DAP did not irreversibly alter neuromuscular function under these conditions (Figure 1, B and D). These data suggest that 3,4-DAP enhanced neuromuscular function in intoxicated diaphragms by restoring threshold levels of acetylcholine release to paralyzed end-plates.

Single-dose 3,4-DAP transiently reverses respiratory depression and paralysis in mice lethally intoxicated with BoNT/A. The ability of 3,4-DAP to restore phrenic end-plate function to paralyzed diaphragms suggested that it would mitigate respiratory depression in vivo. To develop a 3,4-DAP treatment paradigm for respiratory botulism, we first determined no-adverse effect levels for 3,4-DAP doses in naive mice (Supplemental Figure 1; supplemental material available online with this article; https://doi.org/10.1172/jci.insight.132891DS1). Mild systemic effects emerged with low frequency at 8 mg/kg 3,4-DAP (e.g., hypersalivation, behavioral changes, and unsteady gait) and became prevalent at 16 mg/kg, consistent with clinical safety studies indicating acute toxicity at human-equivalent doses (47). Based on these data, subsequent studies were conducted at 2 mg/kg 3,4-DAP, which was well tolerated in naive mice. This dose is the murine allometric equivalent of a clinical 20 mg oral dose (48, 49). Pharmacokinetic (PK) analysis of 3,4-DAP plasma levels after s.c. administration demonstrated rapid absorption and distribution, with an estimated maximum plasma concentration (C_{max}) of 821 ng/mL at 8.4 minutes and terminal phase half-life of 29.4 minutes (Supplemental Figure 2, A and B). Additional PK parameters are summarized in Supplemental Figure 2C.

The therapeutic effects of 3,4-DAP on toxic signs of respiratory botulism were first tested in mice challenged with 2 LD_{50} BoNT/A. Mice exhibited severe symptoms of botulism within 16–20 hours, including paradoxical abdominal breathing, agonal respiration pattern, and generalized muscle paralysis (50). The recruitment of accessory respiratory muscles to support ventilation is a characteristic response to severe diaphragm weakness and manifests in botulism as abdominal paradox, followed by agonal breathing (46, 51). Thus, reversal of abdominal paradox concomitant with reduction in agonal respiratory pattern indicates the resumption of diaphragm function. At the time of 3,4-DAP treatment, the mean clinical severity score (CSS) was 8.2 ± 0.5 and mean breaths per minute (bpm) was reduced to 41.3% ± 4.6% of preintoxication bpm (185.4 ± 6.4 bpm to 76.5 ± 6.5 bpm; $n = 14$, $P < 0.0001$, Welch's t test). S.c. administration of 3,4-DAP rapidly resulted in reduced CSS, reversal of agonal respiration (Figure 2, A and C), and improvement in respiratory rate to 81.5% of preintoxication levels (Figure 2B). Mouse mobility was significantly improved within 0.5 hours of 3,4-DAP treatment (Supplemental Videos 1 and 2, and Figure 2, D and E). However, the effects from a single 3,4-DAP administration were transient. CSS and respiratory rate returned to baseline intoxicated levels between 1.5 and 2 hours after treatment, while mobility remained significantly improved through 2 hours. Correlation of physiological effects with 3,4-DAP plasma levels suggested that symptomatic benefits receded once plasma levels decreased below 25–50 ng/mL (Supplemental Figure 2A). In comparison, a 20-mg oral dose results in a C_{max} of 30–200 ng/mL 3,4-DAP in humans (47), suggesting that 3,4-DAP reversed botulism symptoms at clinically acceptable exposure levels.

3,4-DAP treatment restores respiration and extends survival in terminal BoNT/A-induced respiratory botulism. Because a single dose of 3,4-DAP had transient effects on botulism symptoms, we next evaluated the effects

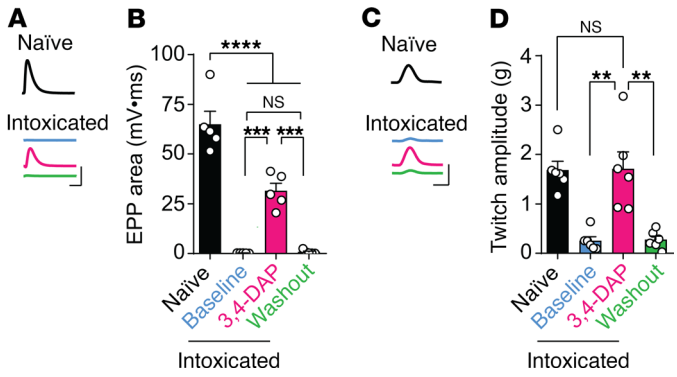

Figure 1. 3,4-DAP restores end-plate potentials and twitch contractions in isolated hemidiaphragms following in vivo intoxication with 2 LD_{50} BoNT/A. Nerve-diaphragm units were removed from naive or BoNT/A-intoxicated mice, divided into hemisections, and separately analyzed for synaptic function or twitch contraction strengths before and after bath addition of 3,4-DAP (10 μM). (**A**) Representative EPP traces from naive diaphragm and BoNT/A-intoxicated diaphragm before and after 3,4-DAP addition. Each trace is the average of 20 EPPs recorded from a single end-plate. Scale bar: 20 mV × 5 ms. (**B**) A comparison of EPP areas in intoxicated hemidiaphragms before and after 3,4-DAP addition (n = 5 diaphragms). EPP areas from naive hemidiaphragms are shown for comparison (n = 5 diaphragms, $n \geq 10$ end-plates per diaphragm). In intoxicated hemidiaphragms, EPP areas were determined from baseline end-plate recordings made prior to addition of 3,4-DAP ($n \geq 10$ end-plates per diaphragm), in the presence of 3,4-DAP ($n \geq 15$ end-plates per diaphragm), and after 3,4-DAP washout ($n \geq 10$ end-plates per diaphragm). Comparisons among mean EPP areas were made by ordinary 1-way ANOVA with Tukey's multiple comparisons test (F = 64.4, $P < 0.0001$). (**C**) Representative twitch traces from naive diaphragm and BoNT/A-intoxicated diaphragm before and after 3,4-DAP addition. Each trace is the average of 6 consecutive twitches from a single diaphragm. Scale bar: 2 g × 30 ms. (**D**) Average twitch contraction strengths in naive and intoxicated diaphragms (n = 6 each). Statistical comparisons were made using ordinary 1-way ANOVA with Tukey's multiple comparisons test (F = 16.8, $P < 0.0001$).

of multiple-dose 3,4-DAP treatments on respiratory function and survival in vivo. These studies were conducted in mice intoxicated by BoNT serotypes A, B, and E, which are historically responsible for over 99% of clinical cases of botulism in the United States (43). Multiple-dose trials were conducted in metabolic cages, allowing for the automated quantitation of oxygen consumption (VO_2) as a surrogate measure of respiratory function (52). Preliminary studies confirmed that lethal intoxication with each serotype consistently resulted in a steady decline in VO_2 that culminated in death (Supplemental Figure 3, A–C). VO_2 decline emerged secondary to clinical indications of respiratory depression and, thus, was considered to represent the terminal stage of respiratory botulism (Supplemental Figure 3D). Mice coadministered 1.5 LD_{50} BoNT/A with neutralizing antitoxin did not develop toxic signs of botulism, confirming that respiratory depression was attributable to botulism (Supplemental Figure 3, A–C). Finally, s.c. administration of 3,4-DAP significantly increased VO_2 in naive mice versus vehicle, confirming physiological effects of 3,4-DAP at the target dose (Supplemental Figure 3, E and F).

To quantify the effects of repeated 3,4-DAP treatments on BoNT/A-induced respiratory botulism, mice intoxicated with 1.5 LD_{50} BoNT/A were administered 8 s.c. injections of 2 mg/kg 3,4-DAP or vehicle at 90-minute intervals. PK modeling suggested that this dosing strategy would sustain 3,4-DAP plasma levels above 50 ng/mL without significantly increasing C_{max} (Supplemental Figure 2D). Based on preliminary studies comparing median time-to-death (TD_{50}) with onset of VO_2 decline, we started treatment once average VO_2 declined below 50% of resting VO_2. At the start of treatment, the actual VO_2 levels were 33.8% ± 4.5% of resting VO_2 (Figure 3A). VO_2 increased in response to each 3,4-DAP treatment, with peak VO_2 values occurring 17–34 minutes after each injection (Figure 3B). In comparison, vehicle had no observable effect on VO_2 levels. Average peak VO_2 measured across all 3,4-DAP treatments was 88.3% ± 2.2% of resting VO_2 (Table 1), although peak VO_2 is likely to be underestimated because of the sparse sampling frequency (once every 17 minutes). 3,4-DAP–treated mice survived for a median of 6.9 hours after the final treatment, with no mice dying prior to the completion of treatment. In contrast, vehicle-treated mice were deceased by the seventh treatment (Figure 3C). 3,4-DAP treatment significantly improved survival and prolonged TD_{50} compared with vehicle-treated mice (Table 1).

To determine whether 3,4-DAP was effective at higher toxin doses, the effects of 8 consecutive 3,4-DAP treatments on VO_2 and survival were evaluated in mice intoxicated with 5 LD_{50} BoNT/A. VO_2 levels declined rapidly after intoxication, consistent with dose-dependent symptomatic onset (53). Treatment was initiated when mean VO_2 was 36.8% ± 3.0% of resting VO_2 (Figure 3D). VO_2 significantly increased

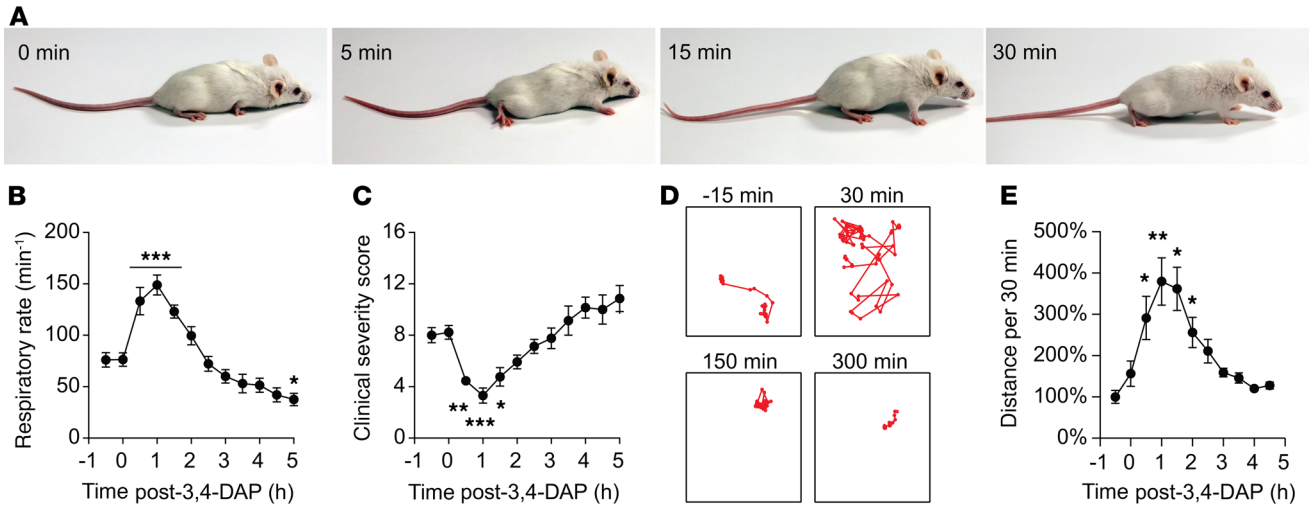

Figure 2. Single administration of 3,4-DAP transiently reverses severe physiological symptoms of botulism. Mice were intoxicated with 2 LD_{50} BoNT/A and administered 3,4-DAP 16–20 hours later, when they presented with severe clinical signs of respiratory depression and neuromuscular weakness (n = 14). (**A**) Images demonstrating longitudinal changes in physiological appearance following 3,4-DAP treatment. Note transition from generalized muscle weakness and severe abdominal paradox to mice that are erect and ambulatory with reduced abdominal paradox. (**B**) Effects of 3,4-DAP treatment on respiratory rate (measured as breaths per minute; bpm). (**C**) Effects of 3,4-DAP treatment on clinical severity scores. (**D**) Representative trajectories reflecting total mouse mobility in 30-minute bins. Presented times represent the midpoint of each bin. (**E**) Grouped effects of 3,4-DAP treatment on overall mobility. Mouse mobility was summed across 30-minute bins to match clinical data and normalized to the 30-minute bin prior to 3,4-DAP treatment. Time points represent the start of each bin. For **B**, **C**, and **E**, statistical comparisons were made to mean values collected 30 minutes prior to 3,4-DAP administration using 1-way repeated measures ANOVA with Dunnett's multiple comparisons test.

following each 3,4-DAP administration to a mean peak VO_2 of 32.3% ± 3.4% (Figure 3E and Table 1). Despite the comparatively modest effect of 3,4-DAP on mean VO_2 in the 5 LD_{50} model, 3,4-DAP improved survival and prolonged TD_{50} (Table 1). 3,4-DAP–treated mice survived a median of 1.5 hours after the final treatment, with only 1 mouse dying during the treatment period. In contrast, vehicle-treated mice were deceased by the fifth treatment (Figure 3F).

Since multiple dosing significantly prolonged survival at both 1.5 and 5 LD_{50} challenges, we next tested survival over longer treatment periods. For this study, we chose an intermediate toxin challenge (3 LD_{50} BoNT/A) and administered 15 consecutive treatments of 3,4-DAP or vehicle at 1.5-hour intervals. This treatment strategy was well tolerated in naive mice, with no evidence of adverse effects (Supplemental Figure 1). Treatment was initiated when mean VO_2 was 31.0% ± 2.9% of resting VO_2 (Figure 3G). VO_2 increased after each 3,4-DAP injection, producing a mean peak VO_2 that was 54.7% ± 2.3% of resting VO_2 (Figure 3H and Table 1). 3,4-DAP–treated mice survived for a median 4.5 hours after the final treatment, with no mice dying during the treatment period. In contrast, vehicle-treated mice were deceased by the sixth treatment (Figure 3I).

Comparison of average peak VO_2 values among the first eight 3,4-DAP treatments in the 1.5, 3 (59.6% ± 3.5%), and 5 LD_{50} BoNT/A challenges revealed an inverse relationship between toxin dose and mean peak VO_2 (linear regression, R^2 = 0.88; F = 155.0, P < 0.0001 versus zero-slope), consistent with ex vivo studies indicating that 3,4-DAP effects are limited by the severity of intoxication (24).

3,4-DAP is effective against serotypes A, B, and E when administered at times of partial paralysis. In contrast to BoNT/A studies, 3,4-DAP was administered immediately upon VO_2 depression after intoxication with serotypes B and E. This was to compensate for the rapid progression of disease in BoNT/E-intoxicated mice (Supplemental Figure 3D) and because preliminary studies showed no efficacy at later treatment times for BoNT/B (not shown). However, 3,4-DAP had no effects on VO_2 or survival in mice intoxicated with serotype B (Figure 4, A–C, and Table 1) or serotype E (Figure 4, D–F, and Table 1). This was surprising, in light of ex vivo findings that 3,4-DAP restored neurotransmission and increased muscle contraction in diaphragms partially intoxicated by both serotypes (24). Thus, we hypothesized that 3,4-DAP would be effective in reversing serotype B– or E–induced botulism toxic signs if administered to less severely intoxicated mice. To test this hypothesis, 3,4-DAP was evaluated following injection of serotypes A, B, or E into the right anterior gastrocnemius muscle at doses that caused paralysis of both gastrocnemius muscles and respiratory muscles, thereby allowing the simultaneous evaluation of 3,4-DAP on multiple muscle groups at different stages of paralysis.

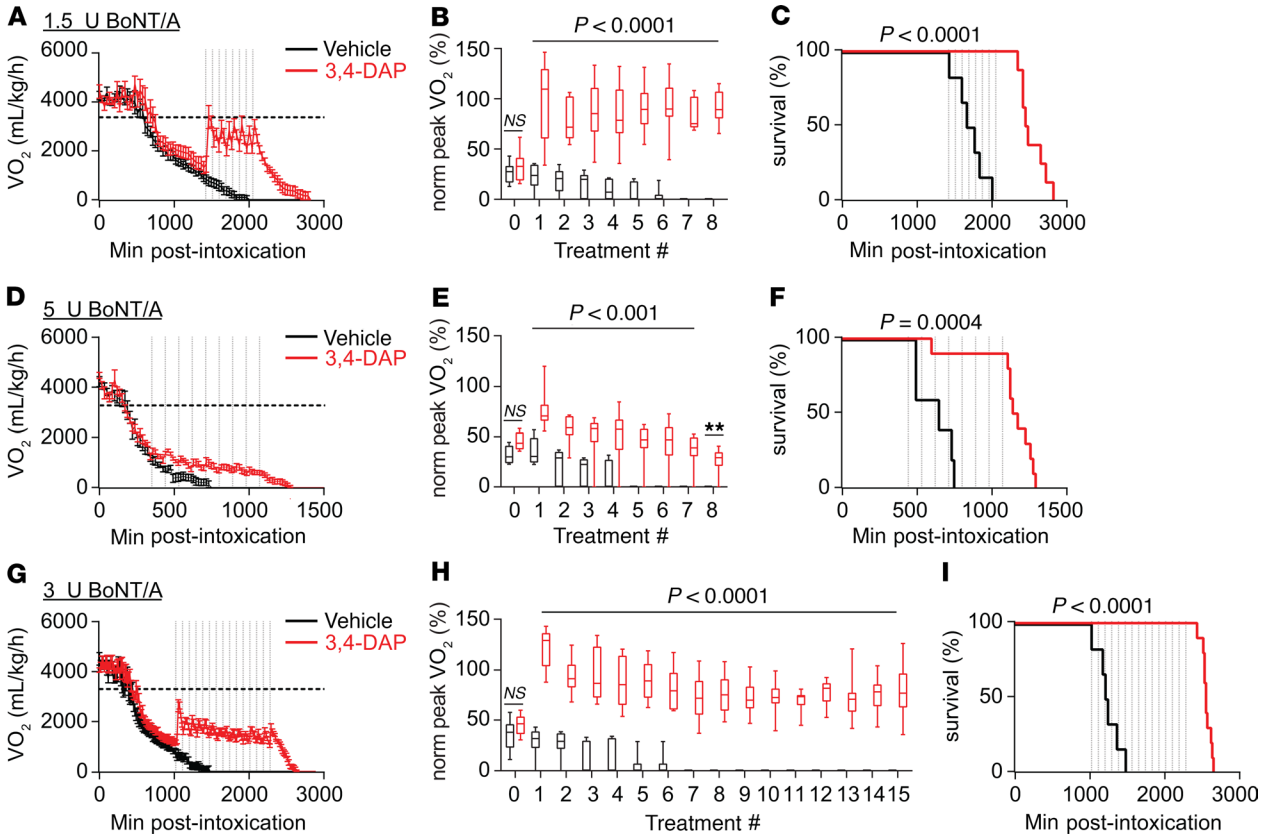

Figure 3. Multiple-dose administration of 3,4-DAP improves oxygen consumption and survival during terminal stages of BoNT/A-induced respiratory botulism in mice. Mice were intoxicated with 1.5 LD_{50}, 3 LD_{50}, or 5 LD_{50} BoNT/A, and 3,4-DAP (2 mg/kg) or vehicle was administered at 90-minute intervals, as represented by vertical dashed lines. (**A**, **D**, and **G**) Longitudinal changes in VO_2 measured before and after 8 or 15 administrations of vehicle or 3,4-DAP. Horizontal dashed lines represent experimentally determined resting VO_2 for purposes of comparison. (**B**, **E**, and **H**) Comparisons of mean peak VO_2 measured between 17 and 51 minutes after 3,4-DAP or vehicle administration. Mean peak VO_2 values were normalized to resting VO_2 values to indicate how effective each treatment of 3,4-DAP was in restoring baseline oxygen consumption. Statistical comparisons were made using 2-way repeated measures ANOVA with Sidak's multiple comparisons test. $^{**}P < 0.01$. (**C**, **F**, and **I**) Kaplan-Meier survival curves were compared using log rank tests for significance between 3,4-DAP and vehicle. Vertical dashed lines represent treatment with vehicle or 3,4-DAP. The number of mice in each experimental group is summarized in Table 1.

Intramuscular administration of 0.7 LD_{50} of serotype A, 0.7 LD_{50} of serotype B, or 1.2 LD_{50} of serotype E produced complete gastrocnemius paralysis (Figure 5, A–C, measured using digit abduction scores [DAS]) and moderate-to-severe abdominal paradoxical breathing (Figure 5, G–I), without causing lethality. Reduction of VO_2 was not observed in pilot studies (not shown); thus, these studies did not evaluate VO_2. 3,4-DAP or vehicle was administered by s.c. injection at the time of maximum observed toxic effects (3 days for serotypes A and B) and during recovery (7 days for serotypes A and B), and the effects on respiratory signs and DAS were evaluated over 4.5 hours (Figure 5, D, E, J, and K). This strategy allowed evaluation of 3,4-DAP effects on respiratory and gastrocnemius muscle function at peak paralysis, as well as during recovery from paralysis. Serotype E has an extremely short duration of effect; therefore, 3,4-DAP was administered at 1 and 2 days after intoxication (Figure 5, F and L), which were the only time points where significant DAS and respiratory symptoms were observed.

Consistent with the more severe paralysis of gastrocnemius muscles, respiratory function recovered more rapidly than gastrocnemius function for all serotypes (Figure 5, G–I, versus Figure 5, A–C). As predicted, 3,4-DAP was least effective in more paralyzed muscles. For example, 3,4-DAP did not improve DAS at 3 days after intoxication with serotypes A or B, but it did improve DAS at 7 days for both serotypes (Figure 5, D and E). Similarly, 3,4-DAP was only effective at 2 days in BoNT/E-intoxicated gastrocnemius muscles (Figure 5F). In comparison, 3,4-DAP reversed respiratory paralysis at all times, independently of serotype (Figure 5, J–L). Under most circumstances, therapeutic benefit fully resolved by 3.5 hours after 3,4-DAP administration. Collectively, these findings demonstrated that 3,4-DAP reversed neuromuscular paralysis caused by multiple BoNT serotypes, with greatest efficacy under conditions of partial paralysis.

Table 1. Summary of TD_{50} values, percent survival at time of last treatment, and peak VO_2 values averaged across all treatments per condition

Serotype: Dose (no. of treatments)	TD_{50} (h)		% Survival at last treatment (survivors/total)		Normalized peak VO_2 (% of resting VO_2)	
	Vehicle	3,4-DAP	Vehicle	3,4-DAP	Vehicle	3,4-DAP
A: 1.5 U (8)	28.6	**41.1**[A]	0% (0/8)	**100% (8/8)**[A]	9.4 ± 3.1	**88.3 ± 2.2**[A]
A: 3.0 U (15)	20.4	**42.5**[A]	0% (0/6)	**100% (10/10)**[A]	3.9 ± 1.7	**54.7 ± 2.3**[A]
A: 5.0 U (8)	10.8	**19.3**[A]	0% (0/6)	**90% (9/10)**[A]	6.8 ± 3.0	**32.3 ± 3.4**[A]
B: 1.5 U (8)	31.0	27.6	60% (3/5)	70% (7/10)	68.0 ± 8.1	72.1 ± 8.5
E: 1.25 U (8)	12.8	11.9	0% (0/6)	0% (0/10)	29.3 ± 5.6	30.0 ± 2.1

Statistically significant differences compared with vehicle are presented in bold. Data were analyzed using log rank tests of Kaplan-Meier survival curves for TD_{50} comparisons, Fisher's exact test for survival proportions, and 2-way repeated measures ANOVA with Sidak's test for normalized peak VO_2. [A]$P < 0.001$.

Discussion

BoNT represents a significant public health challenge. In addition to being an endemic foodborne threat, the toxin is considered to have high risk of deliberate misuse because it is easy to produce and distribute, highly potent, and difficult to treat (54, 55). The current treatment paradigm for suspected botulism exposure (antitoxin infusion and sustained intensive supportive care) is resource intensive and poorly suited to mass casualty scenarios. Furthermore, the limited ability of antitoxin to prevent respiratory depression and collapse in symptomatic patients further complicates treatment strategies, particularly given the limited availability of intensive care facilities (13). If an intraneuronal antidotal treatment were developed, recovery from neuromuscular paralysis would still be delayed until SNARE proteins were regenerated, which will require days of respiratory support (56, 57). Thus, treatments that promote respiratory function in botulism patients will continue to be a critical element of any comprehensive therapeutic strategy. Here, we tested the potential of 3,4-DAP to treat respiratory and skeletal muscle paralysis in murine models of lethal and sublethal botulism caused by BoNT serotypes A, B, and E.

It has long been hypothesized that aminopyridines could reverse botulism symptoms by enhancing acetylcholine release (22). Indeed, ex vivo studies support a therapeutic effect for aminopyridines on skeletal muscle paralysis (22, 39, 58). However, clinical studies involving a small number of patients exposed to different BoNT serotypes, at different doses, and at different stages of disease have proven highly inconsistent, leading to uncertainty about therapeutic potential of aminopyridines (37, 38, 41, 59, 60). In addition to variability in preclinical and clinical studies, additional concerns about 3,4-DAP include the potential for adverse effects, lack of USA Food and Drug Administration (FDA) approval, and uncertainties about effective doses in reversing botulism symptoms (26, 60). The in vivo studies presented here address these concerns by demonstrating that the efficacy of 3,4-DAP is determined by the extent of paralysis and the serotype involved. Furthermore, our results suggest that 3,4-DAP promotes symptomatic benefit at clinically acceptable levels without causing adverse effects.

3,4-DAP was particularly effective in treating respiratory paralysis caused by BoNT/A intoxication. Under physiological conditions, BoNT/A-cleaved SNAP25 ($SNAP25_{197}$) is recruited to synaptic vesicle fusion assemblies, where it primarily exerts an inhibitory role on vesicle release (61, 62). In contrast to other BoNT serotypes, biochemical and cell-based assays reveal that $SNAP25_{197}$ remains capable of supporting vesicle release, albeit with diminished efficiency in comparison with intact SNAP25 (63–65). Consistent with this finding, treatments that increase the probability of synaptic vesicle release — such as voltage-gated Ca^{2+} channel agonists; 3,4-DAP; or elevated extracellular Ca^{2+} levels — can restore synaptic function to cultured neurons and phrenic nerve–diaphragm preparations silenced by BoNT/A but not by other serotypes (24, 42, 66). The selective ability of 3,4-DAP to restore release at BoNT/A-paralyzed end-plates may explain its robust effects at terminal stages of BoNT/A-induced respiratory botulism in comparison with serotypes B and E (24).

3,4-DAP improves respiratory function and prolongs survival in mice challenged with 1.5–5 LD_{50} BoNT/A. However, 3,4-DAP appeared less effective at enhancing VO_2 at the end of each treatment series than at the beginning. While this could indicate a tolerance to 3,4-DAP, such an effect has not been reported previously, to our knowledge. Alternatively, since 3,4-DAP was administered during onset of respiratory paralysis, peak VO_2 levels would be expected to progressively decline until paralysis reached a steady state corresponding to the point of maximal toxic effect. Interestingly, peak VO_2 responses appeared stable over the final 8 doses of

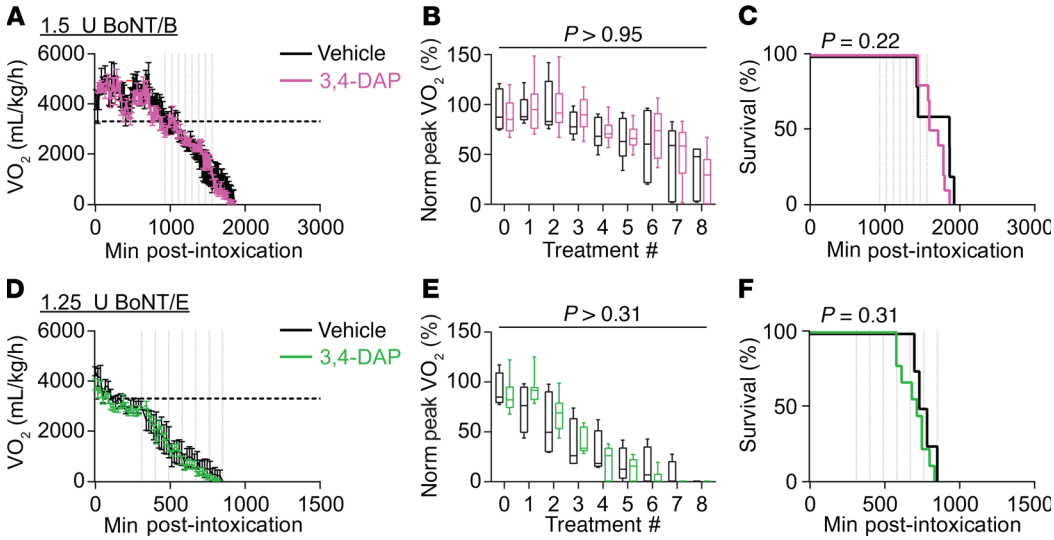

Figure 4. 3,4-DAP does not improve VO_2 or survival during terminal stages of BoNT/B- and BoNT/E-induced respiratory botulism in mice. Mice were intoxicated with 1.5 LD_{50} BoNT/B or 1.25 LD_{50} BoNT/E and 3,4-DAP (2 mg/kg), or vehicle was administered at 90-minute intervals, as represented by vertical dashed lines. (**A** and **D**) Longitudinal changes in VO_2 measured before and after 8 administrations of vehicle or 3,4-DAP. Horizontal dashed lines represent experimentally determined resting VO_2 for purposes of comparison. (**B** and **E**) Comparisons of mean peak VO_2 measured between 17 and 51 minutes after each 3,4-DAP or vehicle administration revealed no significant effect of 3,4-DAP at any time point. Two-way repeated measures ANOVA with Sidak's multiple comparisons test were used. (**C** and **F**) Log rank (Mantex-Cox) tests reveal no differences in Kaplan-Meier survival curves between 3,4-DAP and vehicle for BoNT/B or BoNT/E. The number of mice in each experimental group is summarized in Table 1.

the 24-hour multiple-dosing study (Figure 3C), suggesting that the progression of respiratory paralysis had stabilized. The putative ability of 3,4-DAP to sustain acute survival at the time of maximum respiratory paralysis suggests that chronic treatment may promote long-term survival from BoNT/A botulism.

In contrast to the robust efficacy in BoNT/A-intoxicated mice, 3,4-DAP had no effect on VO_2 or survival in mice intoxicated with serotypes B or E. These findings appeared inconsistent with ex vivo data (24), as well as with a clinical study in which 3,4-DAP was effective in treating a confirmed case of serotype B botulism (41). However, the failure of 3,4-DAP to improve VO_2 in serotype B– or E–intoxicated mice can be explained if late stages of respiratory botulism involve the total paralysis of respiratory end-plates (24). Indeed, in Figure 1, we found that diaphragms collected from mice displaying paradoxical abdominal and agonal breathing had near-complete neurotransmission failure. This hypothesis has the additional implication that 1 or more accessory respiratory muscles (e.g., intercostals or abdominal muscles) can transiently sustain respiratory function following total diaphragm paralysis. Currently, the relative sensitivities of respiratory muscle groups to BoNT are unknown.

In contrast to the inability of 3,4-DAP to treat terminal stages of respiratory botulism caused by serotype B or E, 3,4-DAP was effective in reversing partial respiratory depression following sublethal intoxication for all 3 serotypes. 3,4-DAP also reversed moderate gastrocnemius paralysis during the recovery phase, independent of serotype, but had little effect on gastrocnemius function at peak paralysis. These results are consistent with mechanistic studies demonstrating that 3,4-DAP's primary effect in the nerve terminal is to enhance release probability (24). Thus, in addition to exhibiting specific potency against BoNT/A-induced respiratory botulism, 3,4-DAP is most effective under conditions of partial intoxication by any serotype, when nerve terminals contain both intact and impaired release sites (24). For example, 3,4-DAP has potential to be highly effective in treating symptoms of sublethal and low-dose intoxications. Following high-dose intoxications, 3,4-DAP is anticipated to be effective during symptomatic onset, when patients exhibit respiratory depression but not complete respiratory failure (as demonstrated in Figures 2 and 3), and during recovery from paralysis, as increasing numbers of release sites become available to undergo fusion over a period of weeks to months (e.g., see Figure 5, A–C). Given this broad temporal window for treatment, we propose that chronic administration of 3,4-DAP will reduce the severity and duration of neuromuscular weakness until patients have fully recovered, with greatest efficacy before and after peak paralysis. This is corroborated

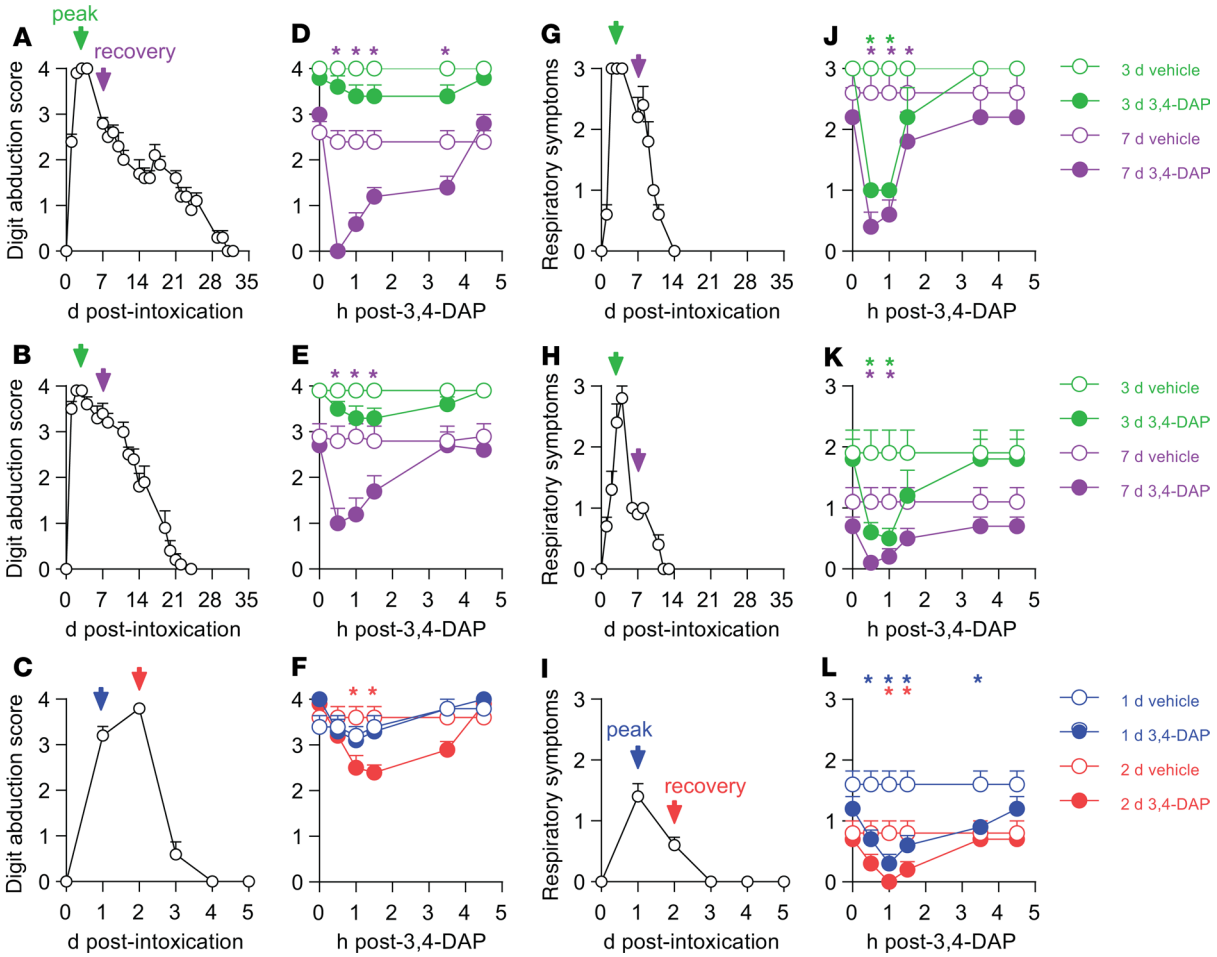

Figure 5. 3,4-DAP has serotype-independent effects on respiratory and skeletal muscle function under conditions of partial paralysis. Mice were administered 0.7 LD_{50} of BoNT/A, 0.7 LD_{50} of BoNT/B, or 1.2 LD_{50} of serotype E into the medial gastrocnemius muscle, and acute effects of vehicle or 3,4-DAP (2 mg/kg, s.c.) on digit abduction scores (DAS) and respiratory signs were monitored over 5 hours. $n = 20$ for each serotype, divided equally into 3,4-DAP and vehicle treatment groups. (**A**–**C**) Mice digit abduction scores were characterized for up to 5 weeks after intoxication with BoNT/A (**A**), BoNT/B (**B**), or BoNT/E (**C**). Arrows depict days on which mice were administered 3,4-DAP or vehicle. The rapid recovery from BoNT/E botulism required that treatments be evaluated on days 1 and 2 after intoxication, as opposed to the 3- and 7-day treatments that were used for the other serotypes. (**D**–**F**) Longitudinal effects of 3,4-DAP or vehicle on DAS. Asterisks indicate time points at which mean DAS were different between vehicle-treated and 3,4-DAP–treated mice. $P < 0.01$, using 2-way repeated measures ANOVA with Sidak's multiple comparisons test. (**G**–**I**) Respiratory signs of botulism were characterized for up to 5 weeks after intoxication with BoNT/A (**G**), BoNT/B (**H**), or BoNT/E (**I**) in the same mice as in **A**–**C**. (**J**–**L**) Longitudinal effects of 3,4-DAP or vehicle on respiratory symptoms. Asterisks indicate time points at which mean respiratory symptoms were different between vehicle-treated and 3,4-DAP–treated mice. $P < 0.01$, using 2-way repeated measures ANOVA with Sidak's multiple comparisons test.

by clinical data showing that 3,4-DAP was effective in treating moderate respiratory symptoms caused by serotypes B (41) and E (60), but did not provide symptomatic relief when administered to fully paralyzed patients requiring long-term mechanical ventilation from BoNT/A botulism (38, 59). Increased neurotransmission in response to chronic 3,4-DAP treatment may also have secondary therapeutic effects on recovery from botulism, such as reducing or preventing neuromuscular atrophy caused by muscle disuse (67).

3,4-DAP is a potentially important adjunct to the FDA-approved heptavalent botulism antitoxin (HBAT). Because the clinical benefit of HBAT is limited to halting progression of botulism rather than speeding recovery, 70% (of 104 cases) of confirmed botulism cases that received HBAT still required mechanical ventilation for a median of 18 days. Furthermore, 89% suffered neurological deficits and/or persistent subjective muscle weakness after discharge (13). Our findings suggest that 3,4-DAP would be particularly effective in mitigating chronic muscle weakness resulting from delayed HBAT administration, thus accelerating overall recovery. Clinically, this would be anticipated to reduce the risk of life-threatening hospital-acquired diseases, decrease treatment costs, and free limited resources for other critical patients (19, 68). 3,4-DAP works orthogonally to HBAT; therefore, the risks of adverse drug interactions are low. BoNT uptake into neurons is

activity dependent (5, 6). Because 3,4-DAP increases compensatory synaptic endocytosis, it is possible that increased synaptic activity would potentiate BoNT/A uptake. However, this effect was not apparent in previous ex vivo studies involving supraphysiological toxin concentrations (24), nor was it observed in comparing disease progression and median times-to-death for serotypes B and E (Figure 4).

The phosphate salt form of 3,4-DAP (Firdapse) is an FDA-approved, first-line symptomatic treatment for Lambert-Eaton myasthenic syndrome (LEMS), which is an autoimmune disease characterized by reduced quantal content and muscle weakness (69). 3,4-DAP is a safe and well-tolerated drug that can be chronically administered without cumulative toxicity; thus, it could be used to treat persistent botulism symptoms (47, 70). The median effective 3,4-DAP plasma concentration for treatment of LEMS is 29.8 ± 10.7 ng/mL, and the approved dose is 10 mg orally, 4 times a day (47). In practice, the dose is adjusted based on the severity of disease and to compensate for differential metabolism of 3,4-DAP (70, 71). Although estimating effective plasma levels from loss of pharmacodynamic effect can be misleading, symptomatic benefit for BoNT/A-induced respiratory botulism occurred at 3,4-DAP plasma concentrations of 25–50 ng/mL, consistent with those used for treatment of LEMS (48, 49). Because the therapeutic mechanism of action of 3,4-DAP is identical for botulism and LEMS, 3,4-DAP may be effective against both diseases at equivalent doses. However, it remains to be determined whether doses that are safe and effective in LEMS will be effective in treating botulism symptoms. Furthermore, while 3,4-DAP is administered orally for LEMS, dysphagia is an early symptom of botulism; thus, oral administration of 3,4-DAP may be initially difficult. Alternatively, since adverse effects of 3,4-DAP appear to be primarily driven by C_{max} as opposed to total drug exposure (Supplemental Figure 2), treatment strategies that reduce C_{max} while maintaining effective plasma levels may improve symptomatic benefit without toxic effects.

Collectively, these data make a compelling preclinical case for use of 3,4-DAP to treat a range of botulism symptoms. While 3,4-DAP is particularly effective in treating serotype A botulism, we have also identified serotype-independent benefits in partially intoxicated muscles. 3,4-DAP has a well-established safety profile and, at approved doses, is unlikely to cause toxic effects if used alone or in combination with HBAT. In light of the recent FDA approval of Firdapse for treatment of LEMS and preliminary clinical evidence of efficacy in mitigating botulism symptoms (37, 41), these studies strongly support further clinical evaluation of 3,4-DAP as a symptomatic treatment for botulism at multiple stages of disease.

Methods

Animals. Female CD-1 mice (8–12 weeks of age; Charles River Laboratories) were group-housed, maintained on a 12-hour diurnal cycle, and provided a standard diet with regular enrichment and water ad libitum. Mice were randomly assigned to groups for all experiments.

Reagents. BoNT serotypes A1 (2.5×10^8 LD_{50}/mg) and B1 (1.1×10^8 LD_{50}/mg) were purchased from Metabiologics Inc. at 10 μg/mL and stored at 4°C. Specific activities for each serotype were confirmed using the mouse i.p. LD_{50} assay (72). Briefly, mouse i.p. lethality was determined for at least 6 doses of each toxin with 5 mice per dose. Survival rates at 96 hours after intoxication were used to calculate LD_{50} values using the probit method. One mouse i.p. LD_{50} was defined as 1 unit (U). BoNT serotype E was purchased from Metabiologics and activated by incubation in 0.05 M sodium phosphate buffer (pH 6.5) with 0.3 mg/mL TripLE trypsin (Sigma-Aldrich) at 37°C for 60 minutes (73). Trypsin was neutralized by addition of 4 volumes of soybean trypsin inhibitor and 10% glycerol, and the activated toxin was aliquoted and stored at –80°C. The LD_{50} of activated toxin was determined to be 3×10^7 LD_{50}/mg. 3,4-DAP (free base) and all components of Tyrode's solution, containing (in mM) 137 NaCl, 5 KCl, 1.8 $CaCl_2$, 1 $MgSO_4$, 24 $NaHCO_3$, 1 NaH_2PO_4, and 11 D-glucose, pH 7.4, were purchased from Sigma-Aldrich. μ-Conotoxin GIIIB was purchased from Alomone Labs and diluted to working concentrations in Tyrode's solution immediately prior to use. Sheep antitoxin against BoNT/A was a gift of Charles Shoemaker (Cummings School of Veterinary Medicine at Tufts University, North Grafton, Massachusetts, USA)

In vivo studies. Mice were administered vehicle or BoNT in physiological saline with 0.2% gelatin (Thermo Fisher Scientific) and 0.3% BSA (Sigma-Aldrich) by i.p. injection. For safety studies, mice were administered 0–16 mg/kg 3,4-DAP by s.c. injection. For efficacy studies, mice were administered 2 mg/kg 3,4-DAP by s.c. injection. Injection sites were varied during multiple-dose administrations to reduce animal distress. Injection of toxin to the right gastrocnemius muscle were performed with a Hamilton syringe in anesthetized mice. To increase validity, every in vivo study included an intoxicated and vehicle-treated cohort.

For VO_2 studies, mice were individually housed in Oxymax CLAMS metabolic caging (Columbus Instruments), and VO_2 and volume of exhaled CO_2 (VCO_2) were measured for 1 minute at 17-minute intervals. Mice were acclimated to metabolic cages for at least 2 days prior to starting studies. The average resting VO_2 of 3306 ± 146 mL/kg/h (mean ± SD, n = 16) was determined by averaging VO_2 levels measured over 4 consecutive days between the hours of 9 am and 3 pm for each mouse and then averaging among mice. Onset of respiratory disease was defined as the point where instantaneous VO_2 first decreased more than 3 SDs below resting VO_2 (e.g., 2868 mL/kg/h), and death was empirically determined to occur once VO_2 dropped below 350 mL/kg/h. Resting VO_2 values remained consistent across all experiments. Multiple-dosing studies in metabolic cages were conducted with 4–8 mice at a time, randomly assigned to vehicle and 3,4-DAP treatment cohorts.

Clinical severity scoring (CSS) was conducted by at least 3 blinded participants. A CSS rubric used in guinea pigs and nonhuman primates was modified to remove ptosis and hypersalivation, which are either absent or difficult to reliably measure in mice (44). The resulting modified CSS rubric was (scores are cumulative): mild abdominal paradox (score of 1), moderate abdominal paradox (score of 2), severe abdominal paradox and/or agonal respiratory pattern (score of 3), lethargy (score of 1), generalized body weakness (score of 2), total body paralysis (lack of righting reflex, score of 3), or death (16). For evaluation of respiratory function in the sublethal botulism model, 3 participants blinded to the treatment groups solely scored respiratory toxic signs on a 0–3 scale.

DAS was used to determine the degree of flaccid muscle paralysis after a local intramuscular injection of BoNT in the right gastrocnemius muscle of mice (74, 75). Briefly, mice were suspended by their tails to elicit a startle response, in which the mouse extends its hind limbs and abducts its hind digits. The spread and pattern of hind digits was assessed using an established scoring system that ranges from 0 (full abduction or movement from the midline from the digit in proximity) to 4 (full paralysis, or inability to abduct any digits). DAS was conducted by 3 participants blinded to the treatment groups.

Automated tracking of mouse activity. Mouse activity was tracked using the markerless pose estimation program DeepLabCut as described (76). Briefly, lethally intoxicated mice were recorded at 30 frames per second for at least 5.5 hours, starting 30 minutes prior to 3,4-DAP treatment. A neural network was trained on mouse features (base of tail and left ear) using 200 video frames with a Quadro M4000 graphics processor (Nvidia). Mouse movement was tracked using the coordinate locations of the trained features, producing a 100% likelihood of accuracy (defined as within 5 μm) in greater than 99.9% of video frames. Distance traveled was initially measured in 5-minute bins. Bins containing greater than 5% of frames with less than a 75% likelihood of accuracy were excluded from analysis (approximately 2% of all bins, primarily corresponding to periods of 3,4-DAP injections). The resulting data were aggregated into 30-minute bins for consistency with clinical scoring data and normalized to the bin collected immediately prior to 3,4-DAP treatment.

PK analysis. For PK analyses, mice (n = 72, average weight 28.6 ± 2.2 g) were randomized into 9 groups and deeply anesthetized using isoflurane prior to (time = 0) or at 5, 10, 20, 40, 60, 120, 240, or 480 minutes after s.c. administration of 2 mg/kg 3,4-DAP (n = 8 per group). Blood was immediately collected by cardiac puncture and spun for 15 minutes at 2000 *g*, and plasma was stored at –80°C until analyzed. 3,4-DAP levels were quantified by standard liquid chromatography tandem mass spectrometry using an Agilent 1290 Infinity liquid chromatograph (Agilent Technologies) with an Ultra Silica 3-μm column (Restek) and a Sciex 6500 QTrap triple quadrupole mass spectrometer (Sciex). The calibration curve was linear over the concentration range of 0.39–1600 ng/mL (r^2 = 0.999). Standard PK parameters were calculated from the relationship between mean plasma concentrations versus time using PKSolver v2.0 (77). Based on the minimum Akaike information criteria (AIC) and visual inspection, a 2-compartment model was selected for PK analyses (78). Area under the concentration time curve was determined using the linear trapezoidal rule.

End-plate recordings. End-plate recordings were conducted as previously described (24). Briefly, mice were deeply anesthetized with isoflurane and immediately decapitated. Diaphragm and associated phrenic nerves were isolated and pinned on a Sylgard dissection dish in oxygenated Tyrode's solution (in mM: 137 NaCl, 5 KCl, 1.8 $CaCl_2$, 1 $MgSO_4$, 24 $NaHCO_3$, 1 NaH_2PO_4, and 11 D-glucose, pH 7.4) at 22°C–24°C. To confirm the preservation of phrenic nerve–diaphragm function, the phrenic nerve was stimulated by a bipolar stimulating electrode (FHC Inc.) with 0.2 ms square-wave pulses with increasing amplitudes (Digitimer) until muscle contraction was observed. Muscle contraction was then selectively blocked by 30-minute incubation with the muscle-specific voltage-gated Na^+ channel blocker μ-conotoxin GIIIB (1–2 μM) (79). Recordings were performed with a Heka EPC10 patch clamp amplifier and sharp glass electrodes (10–20 MΩs) pulled with a Sutter

Instrument P1000. Muscles fibers were impaled close to end-plate junctions, and recordings with starting resting membrane potential (RMP) over –60 mV were discarded. Diaphragms were maintained for no more than 5 hours, with regular exchanges of oxygenated Tyrode's solution.

For each muscle fiber, 20 EPPs were recorded at 0.2 Hz stimulation, followed by a 2-minute recording of mEPPs. At least 10 end-plate recordings per hemidiaphragm were collected under baseline conditions. Intoxicated diaphragms were then incubated in 3,4-DAP (10 μM) for 45 minutes with 0.05 Hz stimulation, and at least 10 end-plate recordings per hemidiaphragm were collected. 3,4-DAP was then washed out by incubating in 37°C oxygenated Tyrode's for 1 hour, and at least 10 end-plate recordings per hemidiaphragm were collected. EPP areas were averaged for each end-plate, corrected for nonlinear summation (80), and averaged among all end-plate recordings per condition per diaphragm. mEPPs were detected with Axograph event detection software (version 1.7.0, Axograph Scientific) from baseline recordings in naive and intoxicated diaphragms.

Myographic recordings. Twitch tension recordings were conducted as previously described (24). Briefly, phrenic nerve–hemidiaphragm preparations were mounted in a 55-mL organ bath system (Radnoti) containing Tyrode's solution at 37°C and continuously bubbled with 95% O_2/5% CO_2. The tissue was allowed to equilibrate for at least 60 minutes with 0.05 Hz stimulation (0.2 ms square voltage pulses at 150% supramaximal voltage) using a Powerlab stimulator (AD Instruments). Force measurements were digitized at a sampling rate of 1000 Hz using Powerlab data acquisition system and recorded and visualized using Labchart version 8 (AD Instruments). Traces were filtered with a 50-Hz digital low-pass threshold to eliminate high-frequency noise. Muscles were discarded as unstable if they displayed greater than 10% variability in tension amplitude during acclimation. Baseline twitch tension was measured for 30 minutes at 0.05 Hz stimulation before 3,4-DAP (10 μM) was added to the bath, and twitch tensions were continuously measured at 0.05 Hz for 60 minutes. 3,4-DAP was washed out by 3 complete media changes, and nerve-elicited twitch tensions were continuously measured at 0.05 Hz for an additional 60 minutes. To determine average responses, the amplitudes of 5 consecutive twitches were averaged for each condition (baseline; 3,4-DAP addition; washout) at the end of each treatment period and then averaged within each group (naive or intoxicated). Representative traces were generated by averaging 5 traces per animal for all animals within a condition.

Statistics. Data are presented as mean ± SEM unless otherwise noted. Binary comparisons between means were made using 2-tailed Student's *t* test with Welch's correction. Multiple means were compared using ordinary 1-way ANOVA with Tukey's multiple comparisons test, 1-way repeated measures ANOVA with Dunnett's multiple comparisons test, or 2-way repeated measures ANOVA with Sidak's multiple comparisons test, as indicated in the text or figure legends. Fisher's exact test was used to compare survival outcomes between paired conditions. Kaplan-Meier survival curves were used to determine TD_{50}, and the log rank (Mantel-Cox) test was used to compare Kaplan-Meier survival curves. $P < 0.05$ was considered significant in all comparisons. Statistical comparisons were made using Prism version 7 (Graphpad Software). Additional details of statistical tests, significance values, and numbers of samples are presented in the results section for nongraphical data or described in the corresponding figure and figure legend.

Study approval. The experimental protocol was approved by the Animal Care and Use Committee at the United States Army Medical Research Institute of Chemical Defense (USDA certificate number 51-F-0006). All procedures were conducted in accordance with the principles stated in the *Guide for the Care and Use of Laboratory Animals* (National Academies Press, 2011).

Author contributions

EVC, JM, BW, MRP, and PM designed experiments. EVC, JM CO, BW, KP, PB, KK, and MRP conducted experiments. All authors analyzed data. EVC, JM, BW, and PM wrote the manuscript.

Acknowledgments

The authors thank Marian Nelson and Megan Lyman for technical assistance and Cindy Kronman for editorial assistance. This work was supported by the Defense Threat Reduction Agency's Joint Science and Technology Office, Medical S&T Division (grant number CB10721), and the National Institute of Allergy and Infectious Diseases (R01 5R01AI093504). This work was performed while JM, CO, and KP held Oak Ridge Institute of Science and Engineering Fellowship awards, EVC held a Geneva fellowship award, and BW held a National Research Council Postdoctoral Fellowship award. The views expressed in this article are those of the authors and do not reflect the official policy of the Department of Army, Department of Defense, or the US Government.

Address correspondence to: Patrick McNutt, USAMRICD, 8350 Ricketts Point Road, Gunpowder, Maryland 21010, USA. Phone: 410.436.8044; Email: patrick.m.mcnutt2.civ@mail.mil.

1. Pirazzini M, Rossetto O, Eleopra R, Montecucco C. Botulinum Neurotoxins: Biology, Pharmacology, and Toxicology. *Pharmacol Rev*. 2017;69(2):200–235.
2. Simpson LL. Identification of the major steps in botulinum toxin action. *Annu Rev Pharmacol Toxicol*. 2004;44:167–193.
3. Peck MW, et al. Historical Perspectives and Guidelines for Botulinum Neurotoxin Subtype Nomenclature. *Toxins (Basel)*. 2017;9(1):E38.
4. Webb RP. Engineering of Botulinum Neurotoxins for Biomedical Applications. *Toxins (Basel)*. 2018;10(6):E231.
5. Dong M, et al. SV2 is the protein receptor for botulinum neurotoxin A. *Science*. 2006;312(5773):592–596.
6. Dong M, Richards DA, Goodnough MC, Tepp WH, Johnson EA, Chapman ER. Synaptotagmins I and II mediate entry of botulinum neurotoxin B into cells. *J Cell Biol*. 2003;162(7):1293–1303.
7. Montal M. Translocation of botulinum neurotoxin light chain protease by the heavy chain protein-conducting channel. *Toxicon*. 2009;54(5):565–569.
8. Burgen AS, Dickens F, Zatman LJ. The action of botulinum toxin on the neuro-muscular junction. *J Physiol (Lond)*. 1949;109(1-2):10–24.
9. Sobel J. Botulism. *Clin Infect Dis*. 2005;41(8):1167–1173.
10. Lindström M, Korkeala H. Laboratory diagnostics of botulism. *Clin Microbiol Rev*. 2006;19(2):298–314.
11. O'Horo JC, et al. Efficacy of Antitoxin Therapy in Treating Patients With Foodborne Botulism: A Systematic Review and Meta-analysis of Cases, 1923-2016. *Clin Infect Dis*. 2017;66(suppl_1):S43–S56.
12. Touman AA, Stratakos GK. Long-Term Complications of Tracheal Intubation. In: Erbay RH, ed. *Tracheal Intubation*. London, United Kingdom: InTechOpen; 2018: 89–112.
13. Yu PA, et al. Safety and Improved Clinical Outcomes in Patients Treated With New Equine-Derived Heptavalent Botulinum Antitoxin. *Clin Infect Dis*. 2017;66(suppl_1):S57–S64.
14. Gottlieb SL, et al. Long-term outcomes of 217 botulism cases in the Republic of Georgia. *Clin Infect Dis*. 2007;45(2):174–180.
15. Simpson L. The life history of a botulinum toxin molecule. *Toxicon*. 2013;68:40–59.
16. Smith T, Roxas-Duncan V, Smith L. Botulinum Neurotoxins as Biothreat Agents. *Journal of Bioterrorism and Biodefense*. 2012;S2:003.
17. Hanig JP, Lamanna C. Toxicity of botulinum toxin: a stoichiometric model for the locus of its extraordinary potency and persistence at the neuromuscular junction. *J Theor Biol*. 1979;77(1):107–113.
18. Tacket CO, Shandera WX, Mann JM, Hargrett NT, Blake PA. Equine antitoxin use and other factors that predict outcome in type A foodborne botulism. *Am J Med*. 1984;76(5):794–798.
19. Souayah N, et al. Trends in outcome and hospitalization charges of adult patients admitted with botulism in the United States. *Neuroepidemiology*. 2012;38(4):233–236.
20. Payne JR, Khouri JM, Jewell NP, Arnon SS. Efficacy of Human Botulism Immune Globulin for the Treatment of Infant Botulism: The First 12 Years Post Licensure. *J Pediatr*. 2018;193:172–177.
21. Richardson JS, et al. Safety and Clinical Outcomes of an Equine-Derived Heptavalent Botulinum Antitoxin Treatment for Confirmed or Suspected Botulism in the United States [published online ahead of print June 15, 2019]. *Clin Infect Dis*. doi:10.1093/cid/ciz515.
22. Lundh H, Leander S, Thesleff S. Antagonism of the paralysis produced by botulinum toxin in the rat. The effects of tetraethylammonium, guanidine and 4-aminopyridine. *J Neurol Sci*. 1977;32(1):29–43.
23. Young DL, Halstead LA. Pyridostigmine for reversal of severe sequelae from botulinum toxin injection. *J Voice*. 2014;28(6):830–834.
24. Bradford AB, Machamer JB, Russo TM, McNutt PM. 3,4-diaminopyridine reverses paralysis in botulinum neurotoxin-intoxicated diaphragms through two functionally distinct mechanisms. *Toxicol Appl Pharmacol*. 2018;341:77–86.
25. Siegel LS, Johnson-Winegar AD, Sellin LC. Effect of 3,4-diaminopyridine on the survival of mice injected with botulinum neurotoxin type A, B, E, or F. *Toxicol Appl Pharmacol*. 1986;84(2):255–263.
26. Mayorov AV, et al. Symptomatic relief of botulinum neurotoxin/a intoxication with aminopyridines: a new twist on an old molecule. *ACS Chem Biol*. 2010;5(12):1183–1191.
27. Adler M, Capacio B, Deshpande SS. Antagonism of botulinum toxin A-mediated muscle paralysis by 3, 4-diaminopyridine delivered via osmotic minipumps. *Toxicon*. 2000;38(10):1381–1388.
28. Thomsen RH, Wilson DF. Effects of 4-aminopyridine and 3,4-diaminopyridine on transmitter release at the neuromuscular junction. *J Pharmacol Exp Ther*. 1983;227(1):260–265.
29. Meriney SD, Lacomis D. Reported direct aminopyridine effects on voltage-gated calcium channels is a high-dose pharmacological off-target effect of no clinical relevance. *J Biol Chem*. 2018;293(41):16100.
30. Delbono O, Kotsias BA. Relation between action potential duration and mechanical activity on rat diaphragm fibers. Effects of 3,4-diaminopyridine and tetraethylammonium. *Pflugers Arch*. 1987;410(4-5):394–400.
31. Lin-Shiau SY, Day SY, Fu WM. Use of ion channel blockers in studying the regulation of skeletal muscle contractions. *Naunyn Schmiedebergs Arch Pharmacol*. 1991;344(6):691–697.
32. Südhof TC, Rizo J. Synaptic vesicle exocytosis. *Cold Spring Harb Perspect Biol*. 2011;3(12):a005637.
33. Morrison VV, Kryzhanovskiĭ GN. [Effect of 4-aminopyridine on the development of experimental botulism]. *Biull Eksp Biol Med*. 1985;100(10):445–447.
34. Morbiato L, Carli L, Johnson EA, Montecucco C, Molgó J, Rossetto O. Neuromuscular paralysis and recovery in mice injected with botulinum neurotoxins A and C. *Eur J Neurosci*. 2007;25(9):2697–2704.
35. Siegel LS, Price JI. Ineffectiveness of 3,4-diaminopyridine as a therapy for type C botulism. *Toxicon*. 1987;25(9):1015–1018.
36. Harris TL, Wenthur CJ, Diego-Taboada A, Mackenzie G, Corbitt TS, Janda KD. Lycopodium clavatum exine microcapsules enable safe oral delivery of 3,4-diaminopyridine for treatment of botulinum neurotoxin A intoxication. *Chem Commun (Camb)*. 2016;52(22):4187–4190.

37. Friggeri A, et al. 3,4-Diaminopyridine may improve neuromuscular block during botulism. *Crit Care*. 2013;17(5):449.
38. Davis LE, Johnson JK, Bicknell JM, Levy H, McEvoy KM. Human type A botulism and treatment with 3,4-diaminopyridine. *Electromyogr Clin Neurophysiol*. 1992;32(7-8):379–383.
39. Simpson LL. A preclinical evaluation of aminopyridines as putative therapeutic agents in the treatment of botulism. *Infect Immun*. 1986;52(3):858–862.
40. Adler M, Macdonald DA, Sellin LC, Parker GW. Effect of 3,4-diaminopyridine on rat extensor digitorum longus muscle paralyzed by local injection of botulinum neurotoxin. *Toxicon*. 1996;34(2):237–249.
41. Dock M, et al. [Treatment of severe botulism with 3,4-diaminopyridine]]. *Presse Med*. 2002;31(13):601–602.
42. Beske PH, Hoffman KM, Machamer JB, Eisen MR, McNutt PM. Use-dependent potentiation of voltage-gated calcium channels rescues neurotransmission in nerve terminals intoxicated by botulinum neurotoxin serotype A. *Sci Rep*. 2017;7(1):15862.
43. CDC. National Botulism Surveillance. http://www.cdc.gov/nationalsurveillance/botulism-surveillance.html.
44. Kodihalli S, et al. Therapeutic efficacy of equine botulism antitoxin in Rhesus macaques. *PLoS ONE*. 2017;12(11):e0186892.
45. Terranova W, Breman JG, Locey RP, Speck S. Botulism type B: epidemiologic aspects of an extensive outbreak. *Am J Epidemiol*. 1978;108(2):150–156.
46. Hughes RA, Bihari D. Acute neuromuscular respiratory paralysis. *J Neurol Neurosurg Psychiatry*. 1993;56(4):334–343.
47. Thakkar N, et al. Population Pharmacokinetics/Pharmacodynamics of 3,4-Diaminopyridine Free Base in Patients With Lambert-Eaton Myasthenia. *CPT Pharmacometrics Syst Pharmacol*. 2017;6(9):625–634.
48. Haroldsen PE, et al. Genetic variation in aryl N-acetyltransferase results in significant differences in the pharmacokinetic and safety profiles of amifampridine (3,4-diaminopyridine) phosphate. *Pharmacol Res Perspect*. 2015;3(1):e00099.
49. Lundh H, Nilsson O, Rosén I, Johansson S. Practical aspects of 3,4-diaminopyridine treatment of the Lambert-Eaton myasthenic syndrome. *Acta Neurol Scand*. 1993;88(2):136–140.
50. Schantz EJ, Kautter DA. Standardized assay for Clostridium botulinum toxins. *Journal of the Association of Official Analytical Chemists*. 1978;61:96–99.
51. Scarlatos A, Welt BA, Cooper BY, Archer D, DeMarse TB, Chau KV. Methods for Detecting Botulinum Toxin with Applicability to Screening Foods Against Biological Terrorist Attacks. *J Food Sci*. 2005;70(8):121–130.
52. Takala J, Keinänen O, Väisänen P, Kari A. Measurement of gas exchange in intensive care: laboratory and clinical validation of a new device. *Crit Care Med*. 1989;17(10):1041–1047.
53. Nishiura H. Incubation period as a clinical predictor of botulism: analysis of previous izushi-borne outbreaks in Hokkaido, Japan, from 1951 to 1965. *Epidemiol Infect*. 2007;135(1):126–130.
54. Arnon SS, et al. Botulinum toxin as a biological weapon: medical and public health management. *JAMA*. 2001;285(8):1059–1070.
55. Thirunavukkarasu N, et al. Botulinum Neurotoxin Detection Methods for Public Health Response and Surveillance. *Front Bioeng Biotechnol*. 2018;6:80.
56. Zanetti G, et al. Botulinum neurotoxin C mutants reveal different effects of syntaxin or SNAP-25 proteolysis on neuromuscular transmission. *PLoS Pathog*. 2017;13(8):e1006567.
57. Cohen LD, et al. Metabolic turnover of synaptic proteins: kinetics, interdependencies and implications for synaptic maintenance. *PLoS ONE*. 2013;8(5):e63191.
58. Adler M, Scovill J, Parker G, Lebeda FJ, Piotrowski J, Deshpande SS. Antagonism of botulinum toxin-induced muscle weakness by 3,4-diaminopyridine in rat phrenic nerve-hemidiaphragm preparations. *Toxicon*. 1995;33(4):527–537.
59. Oriot C, et al. One collective case of type A foodborne botulism in Corsica. *Clin Toxicol (Phila)*. 2011;49(8):752–754.
60. Ball AP, et al. Human botulism caused by Clostridium botulinum type E: the Birmingham outbreak. *Q J Med*. 1979;48(191):473–491.
61. Keller JE, Neale EA. The role of the synaptic protein snap-25 in the potency of botulinum neurotoxin type A. *J Biol Chem*. 2001;276(16):13476–13482.
62. Pellegrini LL, O'Connor V, Lottspeich F, Betz H. Clostridial neurotoxins compromise the stability of a low energy SNARE complex mediating NSF activation of synaptic vesicle fusion. *EMBO J*. 1995;14(19):4705–4713.
63. Lu B. The destructive effect of botulinum neurotoxins on the SNARE protein: SNAP-25 and synaptic membrane fusion. *PeerJ*. 2015;3:e1065.
64. O'Sullivan GA, Mohammed N, Foran PG, Lawrence GW, Oliver Dolly J. Rescue of exocytosis in botulinum toxin A-poisoned chromaffin cells by expression of cleavage-resistant SNAP-25. Identification of the minimal essential C-terminal residues. *J Biol Chem*. 1999;274(52):36897–36904.
65. Fang Q, Zhao Y, Herbst AD, Kim BN, Lindau M. Positively charged amino acids at the SNAP-25 C terminus determine fusion rates, fusion pore properties, and energetics of tight SNARE complex zippering. *J Neurosci*. 2015;35(7):3230–3239.
66. Beske PH, Bradford AB, Hoffman KM, Mason SJ, McNutt PM. In vitro and ex vivo screening of candidate therapeutics to restore neurotransmission in nerve terminals intoxicated by botulinum neurotoxin serotype A1. *Toxicon*. 2018;147:47–53.
67. Salari M, Sharma S, Jog MS. Botulinum Toxin Induced Atrophy: An Uncharted Territory. *Toxins (Basel)*. 2018;10(8):E313.
68. Arnon SS, Schechter R, Maslanka SE, Jewell NP, Hatheway CL. Human botulism immune globulin for the treatment of infant botulism. *N Engl J Med*. 2006;354(5):462–471.
69. Sanders DB. 3,4-Diaminopyridine (DAP) in the treatment of Lambert-Eaton myasthenic syndrome (LEMS). *Ann N Y Acad Sci*. 1998;841:811–816.
70. Lindquist S, Stangel M. Update on treatment options for Lambert-Eaton myasthenic syndrome: focus on use of amifampridine. *Neuropsychiatr Dis Treat*. 2011;7:341–349.
71. Haroldsen PE, Sisic Z, Datt J, Musson DG, Ingenito G. Acetylator Status Impacts Amifampridine Phosphate (Firdapse™) Pharmacokinetics and Exposure to a Greater Extent Than Renal Function. *Clin Ther*. 2017;39(7):1360–1370.
72. Pearce LB, Borodic GE, First ER, MacCallum RD. Measurement of botulinum toxin activity: evaluation of the lethality assay. *Toxicol Appl Pharmacol*. 1994;128(1):69–77.
73. Hubbard KS, Gut IM, Lyman ME, Tuznik KM, Mesngon MT, McNutt PM. High yield derivation of enriched glutamatergic neurons from suspension-cultured mouse ESCs for neurotoxicology research. *BMC Neurosci*. 2012;13:127.
74. Aoki KR. A comparison of the safety margins of botulinum neurotoxin serotypes A, B, and F in mice. *Toxicon*.

2001;39(12):1815–1820.
75. Broide RS, et al. The rat Digit Abduction Score (DAS) assay: a physiological model for assessing botulinum neurotoxin-induced skeletal muscle paralysis. *Toxicon*. 2013;71:18–24.
76. Mathis A, et al. DeepLabCut: markerless pose estimation of user-defined body parts with deep learning. *Nat Neurosci*. 2018;21(9):1281–1289.
77. Zhang Y, Huo M, Zhou J, Xie S. PKSolver: An add-in program for pharmacokinetic and pharmacodynamic data analysis in Microsoft Excel. *Comput Methods Programs Biomed*. 2010;99(3):306–314.
78. Yamaoka K, Nakagawa T, Uno T. Application of Akaike's information criterion (AIC) in the evaluation of linear pharmacokinetic equations. *J Pharmacokinet Biopharm*. 1978;6(2):165–175.
79. Cruz LJ, et al. Conus geographus toxins that discriminate between neuronal and muscle sodium channels. *J Biol Chem*. 1985;260(16):9280–9288.
80. McLachlan EM, Martin AR. Non-linear summation of end-plate potentials in the frog and mouse. *J Physiol (Lond)*. 1981;311:307–324.